

Optical Properties of Isolated Hormone Oxytocin Dianions: Ionization, Reduction, and Copper Complexation Effects

Laure Joly,[†] Rodolphe Antoine,^{*,†} Abdul-Rahman Allouche,[†] Michel Broyer,[†] Jérôme Lemoine,[‡] and Philippe Dugourd[†]

LASIM, UMR 5579, and Sciences Analytiques, UMR 5180, CNRS et Université Lyon 1, Université de Lyon, Villeurbanne, F-69622 Lyon, France

Received: November 25, 2008; Revised Manuscript Received: April 23, 2009

Trapped oxytocin (OT) peptide dianions and copper–oxytocin complex dianions are subjected to electron detachment when irradiated by a UV light. Electron photodetachment experiments as a function of the laser wavelength were performed on the native disulfide-containing ring oxytocin, the reduced dithiol oxytocin, and the Cu^{II}–oxytocin complex. The electron detachment yield was used to monitor the excited electronic spectrum of the trapped ions. The spectra can be used as a fingerprint of the ionization state of the tyrosine chromophore under different structural environments. In gas-phase oxytocin dianion [OT-2H]²⁻, the tyrosine is deprotonated while it is neutral for the reduced form of oxytocin [OT^{SH}-2H]²⁻. Optical spectra for the copper complex dianion [OT-4H+Cu]²⁻ are in favor of a neutral tyrosine in the complex. A structure with the metal cation chelated to four deprotonated amide groups is proposed for this complex.

I. Introduction

Oxytocin (OT) is an important peptide hormone involved in reproductive functions, the primary physiological action of which is to elicit smooth muscle contraction, and thereby milk ejection and uterine contraction in mammals.¹ It has interesting structural features including a 20-member disulfide-containing ring and an acyclic CONH₂-terminal tripeptide moiety (see Scheme 1).

The biological activity of peptide hormones depends on their structural and conformational properties.^{1–5} In the case of oxytocin, conformational studies have been combined with activity studies to obtain better insight into the relationship between structure and activity.⁶ The crystal structure of the oxytocin hormone complexed with its receptor neurophysin protein has been determined, which has permitted elucidation of the key residues that are involved in hormone–receptor recognition.⁷ Moreover, it was shown that the presence of a divalent transition-metal ion (usually Zn²⁺, Ni²⁺, and Co²⁺) dramatically enhances the binding properties of oxytocin to its cellular receptor.⁸ Following this observation, numerous studies, in particular, potentiometric and photospectrometric studies, were performed on metal–OT complexes.^{9–13} The drawback of these experiments is that it is difficult to characterize the exact structure, in particular, the stoichiometry of the complexes whose properties are measured.

By bringing such complexes to the gas phase, it is possible to study complexes with a defined stoichiometry. Electrospray ionization mass spectrometry has been successfully used for transfer to the gas-phase transition-metal ions with oxytocin complexes.^{14–16} A deep understanding of the structural changes induced in OT by divalent metal ion coordination has recently been obtained by coupling mass spectrometry and ion mobility techniques.^{17,18} The formation of a square-planar complex in

which the transition-metal ion is bound to the neutral N-terminal amino group and to three deprotonated amide groups (4N chelation) was proposed.

In this contribution, we use gas-phase optical spectroscopy to evaluate the influence of the sulfide reduction and of the copper complexation on the structure of oxytocin peptide dianions. Trapped oxytocin peptide dianions and copper–oxytocin complex dianions are subjected to electron detachment when irradiated by a UV light. The electron detachment yield was used to monitor the excited electronic spectrum of the trapped ions. The UV spectra provide a direct diagnostic of the ionization state of chromophores,^{19,20} in particular, of the tyrosine residue.²¹

II. Methods

Sample Preparation. Oxytocin was purchased from Sigma-Aldrich (St. Quentin Fallavier, France). Copper salt (CuCl₂) is high-purity crystal grade and solvents are high-performance liquid chromatography grade.

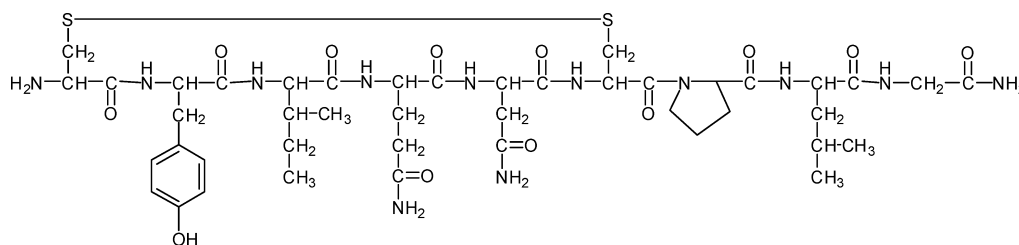
Reduced and Nonreduced OT Solutions. The electrospray solution for OT was prepared by dissolving the peptide (100 μM) in a 1:1 mixture of water and acetonitrile. The reduction of the disulfide bridge of OT, leading to the formation of a dithiol (OT dithiol), was obtained by adding 10 mM dithiothreitol to OT (2 mM) aqueous solution and keeping at room temperature for 12 h. The electrospray solution for the reduced form of oxytocin (OT^{SH}) was then prepared by dissolving the OT^{SH} peptides (100 μM) in a 1:1 mixture of water and acetonitrile. KOH was added to obtain a final solution at pH 5–6. With these conditions, dianions of the form [OT-2H]²⁻ or [OT^{SH}-2H]²⁻ were observed in the negative ion electrospray mass spectrum.

Copper–OT Complexes. The electrospray solution was prepared following ref 17 by dissolving the peptides (50 μM) and the copper salt (50 μM) in a 1:1 mixture of water and acetonitrile. The addition of 1% NH₄OH yielded a pH of 9–10. With these conditions, both the monoanion [OT-3H+Cu]⁻ and the dianion [OT-4H+Cu]²⁻ were observed in the negative ion electrospray mass spectrum.

* To whom correspondence should be addressed. E-mail: rantoine@lasim.univ-lyon1.fr.

[†] LASIM, UMR 5579.

[‡] Sciences Analytiques, UMR 5180.

SCHEME 1: Chemical Structure of Oxytocin (amino-acid sequence Cys-Tyr-Ile-Gln-Asn-Cys-Pro-Leu-GlyNH₂)

Mass Spectrometry, Laser Irradiation of Trapped Ions. The experimental setup²² consists of a commercial LCQ Duo quadrupole ion trap mass spectrometer (ThermoFinnigan, San Jose, CA) coupled to a Panther OPO laser pumped by a 355 nm Nd:YAG PowerLite 8000 (5 ns pulse width, 20 Hz repetition rate). Frequency doubling allows scanning in the 215–330 nm range. The vacuum chamber and the central ring electrode of the mass spectrometer were modified to allow the injection at the center of the trap of UV and visible lights. An electromechanical shutter triggered on the RF signal of the ion trap synchronizes the laser irradiation with the trapping of the ions. The ions are injected into the trap, mass-selected, and then laser-irradiated for 10 laser shots. Fragmentation spectra are systematically recorded as a function of the laser wavelength. The photodetachment yield is given by $\ln((\text{parent} + \text{fragment})/\text{parent})/\lambda/P_1$ where λ is the laser wavelength and P_1 is the laser power.

III. Results and Discussion

Photofragmentation Mass Spectra: Electron Photodetachment and Neutral Losses. The mass spectra obtained following the laser irradiation at 255 nm of the oxytocin dianions in the nonreduced form $[\text{OT}-2\text{H}]^{2-}$, the reduced form $[\text{OT}^{\text{SH}}-2\text{H}]^{2-}$, and that complexed with copper $[\text{OT}-4\text{H}+\text{Cu}]^{2-}$ are displayed in Figure 1. The main fragment observed corresponds to the radical oxidized ion generated by electron detachment from the precursor ion. This photoinduced charge reduction from the precursor ion is the main fragment channel observed for the three dianions. Electron loss was already observed as the main fragmentation channel after UV excitation in polypeptides and DNA polyanions mass spectra.^{23–25} In the near UV, the main electron detachment mechanism is a two-step mechanism. The first step is a resonant electronic excitation of the precursor ion,^{25–27} which is followed by a delayed electron emission.²⁸ At 255 nm, the electronic excitation is mainly due to the $\pi\pi^*$ excitations in oxytocin.

For OT and OT^{SH} dianions, some minor fragments are also observed in the mass spectra (in the m/z range 850–1000 Da). These fragments correspond to neutral losses arising from the fragmentation of the oxidized anion. Neutral losses are due to bond rearrangement processes that follow the photogeneration of the radical oxidized ion.²⁹ The nature of the neutral losses depends on the state of reduction of oxytocin. For OT, losses of 33, 65, and 106 Da are observed, whereas losses of 44 and 70 Da are observed for the reduced form of oxytocin OT^{SH}. The loss of 106 Da arises from the recombination of the radical oxygen of the tyrosine side chain residue. The losses of 33 and 65 Da might correspond to the losses of SH[•] and SSH[•] radicals, as also observed in electron capture dissociation experiments.¹⁴ We have no clear interpretation for the losses observed for the reduced form OT^{SH}. The loss of 44 Da might correspond to the elimination of a [•]CONH₂ radical, for example, by involving in a first step a hydrogen transfer between the C α_5 and a radical site initially located on the S atom of Cys6, and followed by a β - γ cleavage of an Asn5 side chain.

However, we want to emphasize that the characteristic loss of 106 Da, which is a signature of the presence of a tyrosyl radical,²⁹ is inhibited when the oxytocin disulfide bridge is reduced. These differences in neutral loss channels, between OT and OT^{SH}, may reflect the initial position of the radical that is obtained after electron loss and may thus be related to different initial charge location in the peptide (as discussed below).

For OT^{Cu}, no additional fragment corresponding to neutral losses is observed. This inhibition of fragmentation following electron photodetachment is probably due to an increase in the dissociation energies caused by a strong coordination of the copper cation to the peptide.

Electron Photodetachment Yields of the Reduced and Nonreduced Forms of Oxytocin. Signature of the Ionization State of Tyrosine. The electron detachment yields measured for the $[\text{OT}-2\text{H}]^{2-}$ and $[\text{OT}^{\text{SH}}-2\text{H}]^{2-}$ dianions as a function of

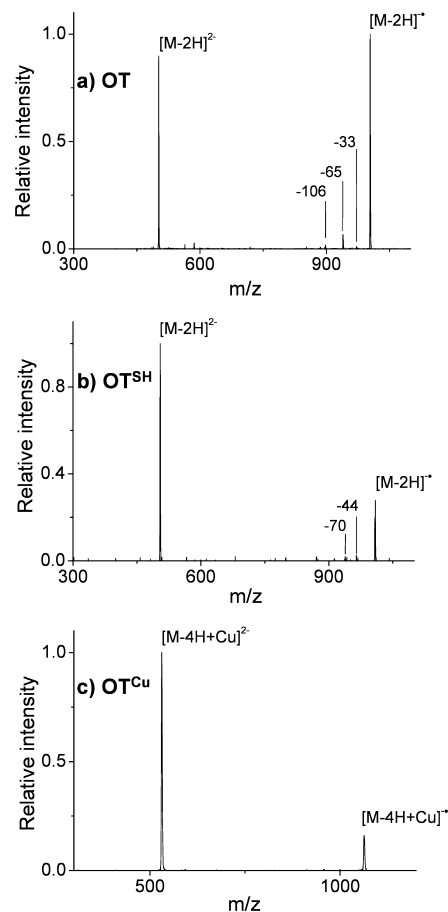


Figure 1. Mass spectra obtained after laser irradiation ($\lambda = 255$ nm) of (a) the doubly deprotonated oxytocin (OT) peptide, (b) the doubly deprotonated dithiol oxytocin (OT^{SH}) peptide, and (c) the copper–oxytocin $[\text{M}-4\text{H}+\text{Cu}]^{2-}$ complex (OT^{Cu}). The irradiation time was 500 ms (10 laser shots), and the laser power was (a) 6.2 mW, (b) 3 mW, and (c) 3.3 mW.

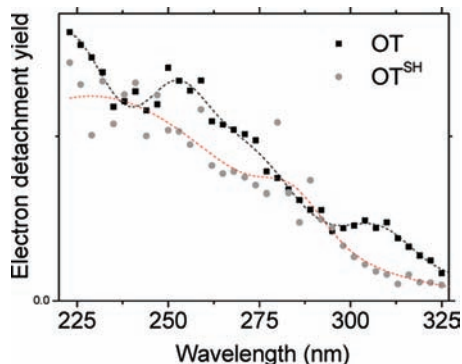


Figure 2. Photodetachment yield measured as a function of the laser wavelength for the doubly deprotonated oxytocin (OT) peptide and the doubly deprotonated reduced dithiol oxytocin (OT^{SH}) peptide. Dashed curves are smoothed curves of the experimental data. The irradiation time was 500 ms (10 laser shots).

the laser wavelength in the 220–325 nm range are shown in Figure 2. For OT^{SH} , the spectrum displays a monotone increase in the absorption from around 315–220 nm, with a shoulder centered around 284 nm. For OT, a different optical spectrum is obtained. A bathochromic shift is observed with an onset of the electron detachment yield occurring at 325 nm. Two bands centered at around 310 and 258 nm are observed. The bathochromic shift, observed between OT^{SH} and OT spectra, is characteristic of the phenolic-OH deprotonation of the tyrosine residue in $[\text{OT}-2\text{H}]^{2-}$ dianions, as already observed for angiotensin dianions²¹ and as confirmed by time-dependent density functional theory (TDDFT) calculations.²¹ The strong bathochromism is due to the destabilization of tyrosine π molecular orbitals caused by the negative charge on the hydroxyl oxygen. According to TDDFT calculations, the band at 258 nm is mainly due to a $\pi-\pi^*$ excitation of the carbonyl bond and the one at 310 nm is mainly due to a $\pi-\pi^*$ excitation of the benzyl ring. The disulfide bridge also contributes to the absorption around 280 and 240 nm.³⁰ For the reduced form of oxytocin, the resonant electronic excitation above 220 nm is mainly due to a $\pi-\pi^*$ excitation of the benzyl ring.

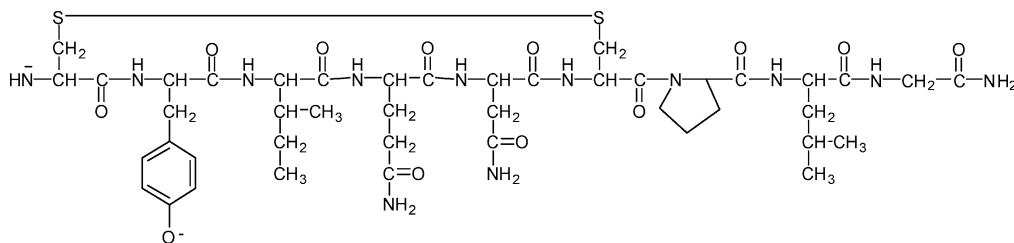
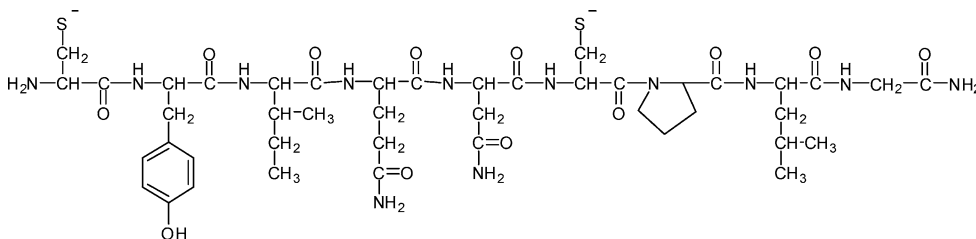
Oxytocin is a peptide without carboxyl groups. The most acidic group in OT is the Tyr2 side chain.¹¹ The first deprotonation site is then expected to be the OH group of Tyr2. As discussed above, this is in agreement with the optical spectrum displayed in Figure 2. The other potential proton donor groups, the $-\text{CONH}-$ backbone amides, the $-\text{CONH}_2$ amides of Gln4, Asn5, and Gly9, and the N-terminal $-\text{NH}_2$ amino group, have significantly higher pK_a values. The pK_a value of the terminal amino group is significantly lowered as compared to those of the other groups³¹ because of the close vicinity of the disulfide group. The second deprotonation may then occur at the terminal amino group. Concerning the reduced form of oxytocin, the presence of the dithiol renders the OT^{SH} peptide more acidic. Indeed, pK_a values for thiols in peptides range from 9.0 to 9.5.³² Thus, deprotonation of the thiol groups in OT^{SH} comes into competition with the deprotonation of the phenolic-OH group. The optical spectrum (see Figure 2) shows that the tyrosine is neutral in OT^{SH} . The deprotonations may thus occur on the two thiol groups, as shown in the following schemes (Schemes 2 and 3). To summarize, the deprotonations in $[\text{OT}-2\text{H}]^{2-}$ occur on the phenolic-OH and probably on the terminal amino group, whereas for $[\text{OT}^{\text{SH}}-2\text{H}]^{2-}$ they occur on the two thiol groups.

Electron Photodetachment Yield of the Copper Metal–Oxytocin Dianion. The electron detachment yields measured for the $[\text{OT}-4\text{H}+\text{Cu}]^{2-}$ dianions as a function of the laser

wavelength in the 220–325 nm range is shown in Figure 3. The spectrum displays a monotone increase in the absorption from around 310 to 220 nm, with shoulder patterns centered around 280 nm and to a lesser extent around 300 nm. The optical spectrum of the copper–oxytocin complex is very similar to the one reported for OT^{SH} dianions (see Figure 2). This similarity may indicate that the tyrosine residue in the $[\text{OT}-4\text{H}+\text{Cu}]^{2-}$ dianions is neutral (see next section).

The conformation of the disulfide bridged peptide hormone oxytocin is ideally suited for metal ion coordination via deprotonated amide nitrogens.¹⁰ It was presently reported that Cu^{II} and Ni^{II} form unusually stable square planar complexes with oxytocin and analogues, with four N coordination (4N complexes) at pH greater than 6.^{9,11,12} In these complexes the metal ion is bound to the neutral N-terminal amino group and to the nitrogen atoms of three deprotonated amide groups (4N chelation). A combination of ion mobility and collision induced dissociation experiments has recently confirmed the formation of 4N complexes in the gas phase.¹⁷ For $[\text{OT}-3\text{H}+\text{Cu}]^-$, structures with a quasi-square planar Cu^{2+} center and a tetradentate ligand (deprotonated amide nitrogen atoms of the C-terminal residues Cys6, Leu8, and Gly9 along with the N-terminal amino group) has been proposed. For $[\text{OT}-4\text{H}+\text{Cu}]^{2-}$ dianions, a similar 4N chelation structure with a deprotonated tyrosine would be a possible structure. However, the present reported optical spectrum for this complex seems to be in favor of a neutral tyrosine. This suggests an alternative structure with the metal cations bound to four deprotonated amide groups as shown in Scheme 4. This type of structure has already been observed in the bis-biuret complex.^{33,34} It is stabilized by electrostatic forces between the cations and deprotonated amide groups and by the delocalization of the negative charges on the peptide bonds over the disulfide-containing ring.

Theoretical Investigation of the Optical Properties of GlyTyrGlyGlyGly Pentapeptide Complexed with Cu^{2+} . Obviously, not only deprotonation of the tyrosine residue but also the presence of the copper cation and of the four negative charges may affect the optical properties of the oxytocin peptide. Unfortunately, computation of copper oxytocin complex excited states is still out of reach. To probe these effects at a high level of theory (TDDFT), we chose a simplified 4N chelation complex composed of a mimic peptide (GlyTyrGlyGlyGly pentapeptide) complexed with Cu^{2+} . In the $\text{GYGGG}^{\text{Cu}}_{\text{A}}$ complex, the tyrosine is deprotonated and three amide nitrogen atoms are deprotonated. In the $\text{GYGGG}^{\text{Cu}}_{\text{B}}$ complex, the tyrosine is neutral and four amide nitrogen atoms are deprotonated. The structures of these two complexes are displayed as insets in Figure 4. Trial 4N chelation structures were first optimized for both complexes, at the MM+ force field level. The lowest energy structures were then reoptimized using the semiempirical PM6 calculations.³⁵ Single-point calculations were then performed for the $\text{GYGGG}^{\text{Cu}}_{\text{A}}$ and $\text{GYGGG}^{\text{Cu}}_{\text{B}}$ complexes, at the density functional method (DFT) with the B3LYP hybrid functional and the 6-31++G** basis set. The $\text{GYGGG}^{\text{Cu}}_{\text{A}}$ complex is found to be slightly more stable by 44 meV compared to the $\text{GYGGG}^{\text{Cu}}_{\text{B}}$ complex. Absorption spectra were obtained from the TDDFT method using B3LYP with 6-31++G** basis set. Although of moderate size, the 6-31++G** basis set contains diffuse functions and usually enables an appropriate description of excited states. For the two complexes, numerous bands with non-negligible oscillator strength are present in the 240–500 nm range. In fact, the presence of both the copper cation and the four deprotonations add some

SCHEME 2: Proposed Structure for [OT-2H]²⁻**SCHEME 3: Proposed Structure for [OT^{SH}-2H]²⁻**

contributions to the optical spectra. In particular, the analysis of orbitals responsible for the transition in the 300–400 nm range indicates that the calculated transitions are mainly due to the 4N chelation ring structure and involve orbitals localized on the copper atom. The analysis of the leading excitations between occupied and virtual Kohn–Sham orbitals participating in the intense transition at 367 nm show that excitation occurs within the 4N chelation structures for the **GYGGG^{Cu}_B** complex. On the other hand, for the **GYGGG^{Cu}_A** complex, the analysis of the intense transition at 349 nm shows that the excitation

is mainly due to a charge transfer between the deprotonated tyrosine and the 4N chelation complex. The **GYGGG^{Cu}_A** complex with the deprotonated tyrosine displays stronger oscillator strengths in the 300–400 nm range than the **GYGGG^{Cu}_B** complex with the neutral tyrosine. In particular, for the **GYGGG^{Cu}_A** mimic complex, no decrease in the absorption is expected between 300 and 350 nm. Experimentally, we do not observe a significant absorption in the 300–325 nm range (see Figure 3) with almost no fragmentation above 310 nm. However, it is difficult to directly compare the calculated spectra of the mimic peptide copper complexes with the experimental spectrum of the OT^{Cu} complex. It should also be pointed out that the transition energies for the states with a long-range charge-transfer character are systematically too low in the framework of the TDDFT approach.³⁶ Furthermore, calculations were performed by including only 400 transitions. This

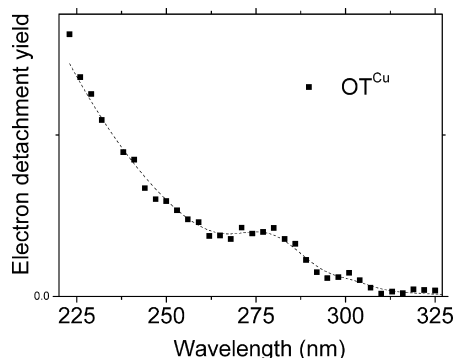


Figure 3. Photodetachment yield measured as a function of the laser wavelength for the copper–oxytocin [M-4H+Cu]²⁻ complex (OT^{Cu}). The dashed curve is a smoothed curve of the experimental data. The irradiation time was 500 ms (10 laser shots).

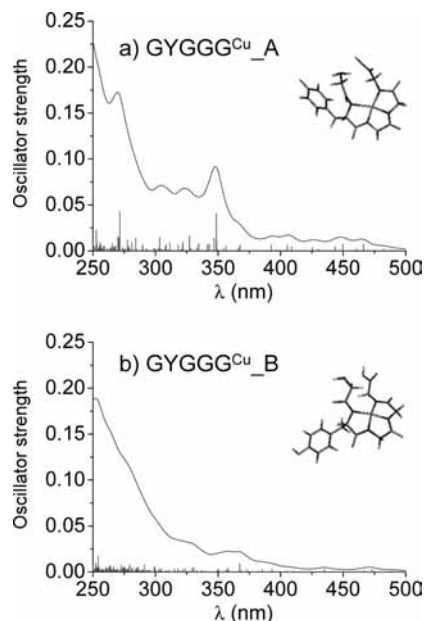
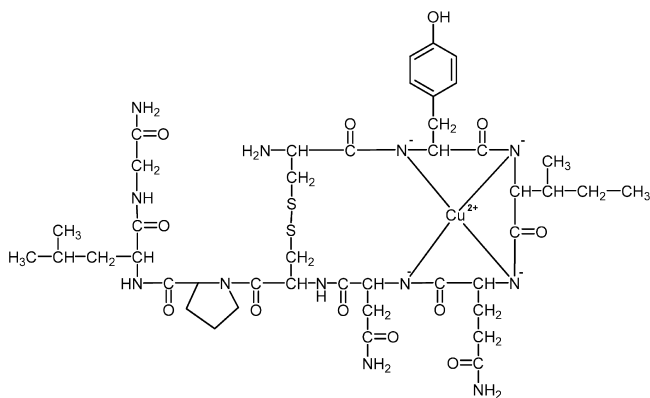
SCHEME 4: Proposed Structure for the OT^{Cu} Complex

Figure 4. TDDFT calculation of the optically allowed transitions λ (in nanometers) and oscillator strengths (f_e) for the **GYGGG^{Cu}_A** (a) and the **GYGGG^{Cu}_B** (b) complexes. The number of transitions (doublet states) included in the calculation is 400. Broadening of the lines is simulated by Lorentzian functions with a width of 7 nm. The lowest energy structures at the DFT level of theory are displayed in the insets.

truncation leads to an underestimation of the total oscillator strength below 250 nm. With these reserves, the calculated spectra confirm that the weak absorption observed for the complex above 300 nm is in favor of a neutral tyrosine residue in the copper–oxytocin complex.

IV. Conclusion

We used electron detachment to report the gas-phase electronic excitation spectra of oxytocin dianions under different structural environments. Experiments provide a clear signature of the ionization state of the tyrosyl group. For the native disulfide-containing ring oxytocin, the phenolic-OH group of tyrosine is deprotonated whereas for the reduced dithiol oxytocin, this group is neutral. The optical spectrum for the Cu^{II}–oxytocin complex dianion is in favor of a neutral tyrosine. A structure, different from the 4N solution structure, with four deprotonated amide groups might be adopted by this complex. This last result highlights the specificity and richness of the chemistry in the gas phase for metal–ligand systems.^{37,38} This new type of chelated structures should now be confirmed by calculations or further experiments.

References and Notes

- Gimpl, G.; Fahrenholz, F. *Physiol. Rev.* **2001**, *81*, 629.
- Breslow, E. *Annu. Rev. Biochem.* **1978**, *48*, 251.
- Fanelli, F.; Barbier, P.; Zanchetta, D.; De Benedetti, P. G.; Chini, B. *Mol. Pharmacol.* **1999**, *56*, 214.
- Slusarz, M. J.; Slusarz, R.; Ciarkowski, J. *J. Pept. Sci.* **2006**, *12*, 171.
- Conner, M.; Hawtin, S. R.; Simms, J.; Wootten, D.; Lawson, Z.; Conner, A. C.; Parslow, R. A.; Wheatley, M. *J. Biol. Chem.* **2007**, *282*, 17405.
- Hruby, V. J. Topics in Molecular Pharmacology. In *Topics in Molecular Pharmacology, Vol. 1*; Burgen, A. N. V., Roberts, G. C. K., Eds.; Elsevier: Amsterdam, 1981.
- Rose, J. P.; Wu, C.-K.; Hsiao, C.-D.; Breslow, E.; Wang, B.-C. *Nat. Struct. Biol.* **1996**, *3*, 163.
- Pearlmutter, A. F.; Soloff, M. S. *J. Biol. Chem.* **1979**, *254*, 3899.
- Bal, W.; Kozłowski, H.; Lammek, B.; Pettit, L. D.; Rolka, K. *J. Inorg. Biochem.* **1992**, *45*, 193.
- Campbell, B. J.; Chu, F. S.; Hubbard, S. *Biochemistry* **1963**, *2*, 764.
- Danyi, P.; Varnagy, K.; Sovago, I.; Schon, I.; Sanna, D.; Micera, G. *J. Inorg. Biochem.* **1995**, *60*, 69.
- Kozłowski, H.; Radomska, B.; Kupryszewski, G.; Lammek, B.; Livera, C.; Pettit, L. D.; Pyburn, S. *J. Chem. Soc., Dalton Trans.* **1989**, 173.
- Chruscinska, E.; Derdowska, I.; Kozłowski, H.; Lammek, B.; Luckowski, M.; Oldziej, S.; Swiatek-Kozłowska, J. *New. J. Chem.* **2003**, *27*, 251.
- Kleinnijenhuis, A. J.; Mihalca, R.; Heeren, R. M. A.; Heck, A. J. R. *Int. J. Mass Spectrom.* **2006**, *253*, 217.
- Wei, H.; Luo, X.; Wu, Y.; Yao, Y.; Guo, Z.; Zhu, L. *J. Chem. Soc., Dalton Trans.* **2000**, 4196.
- Mihalca, R.; van der Burgt, Y. E. M.; Heck, A. J. R.; Heeren, R. M. A. *J. Mass Spectrom.* **2007**, *42*, 450.
- Wyttenbach, T.; Liu, D.; Bowers, M. T. *J. Am. Chem. Soc.* **2008**, *130*, 5993.
- Liu, D.; Seuthe, A. B.; Ehrler, O. T.; Zhang, X.; Wyttenbach, T.; Hsu, J. F.; Bowers, M. T. *J. Am. Chem. Soc.* **2005**, *127*, 2024.
- Lammich, L.; Petersen, M. A.; Nielsen, M. B.; Andersen, L. H. *Biophys. J.* **2007**, *92*, 201.
- Nielsen, S. B.; Lapiere, A.; Andersen, J. U.; Pedersen, U. V.; Tomita, S.; Andersen, L. H. *Phys. Rev. Lett.* **2001**, *87*, 228102.
- Joly, L.; Antoine, R.; Allouche, A. R.; Broyer, M.; Lemoine, J.; Dugourd, P. *J. Am. Chem. Soc.* **2007**, *129*, 8428.
- Talbot, F. O.; Tabarin, T.; Antoine, R.; Broyer, M.; Dugourd, P. *J. Chem. Phys.* **2005**, *122*, 074310.
- Gabelica, V.; Tabarin, T.; Antoine, R.; Rosu, F.; Compagnon, I.; Broyer, M.; De Pauw, E.; Dugourd, P. *Anal. Chem.* **2006**, *78*, 6564.
- Antoine, R.; Joly, L.; Tabarin, T.; Broyer, M.; Dugourd, P.; Lemoine, J. *Rapid Commun. Mass Spectrom.* **2007**, *21*, 265.
- Joly, L.; Antoine, R.; Broyer, M.; Lemoine, J.; Dugourd, P. *J. Phys. Chem. A* **2008**, *112*, 898.
- Weber, J. M.; Ioffe, I. N.; Bernt, K. M.; Löffler, D.; Friedrich, J.; Ehrler, O. L.; Danell, A. S.; Parks, J. H.; Kappes, M. M. *J. Am. Chem. Soc.* **2004**, *126*, 8585.
- Wang, L.-S.; Wang, X.-B. *J. Phys. Chem. A* **2000**, *104*, 1978.
- Matheis, K. T.; Joly, L.; Antoine, R.; Lépine, F.; Bordas, C.; Ehrler, O. T.; Allouche, A.-R.; Kappes, M. M.; Dugourd, P. *J. Am. Chem. Soc.* **2008**, *130*, 15903.
- Antoine, R.; Joly, L.; Allouche, A.-R.; Broyer, M.; Lemoine, J.; Dugourd, P. *Eur. Phys. J. D* **2009**, *51*, 117.
- Carmack, M.; Neubert, L. A. *J. Am. Chem. Soc.* **1967**, *89*, 7134.
- Siegel, H.; Martin, R. B. *Chem. Rev.* **1982**, *82*, 385.
- Creighton, T. E. *Proteins*; W.H. Freeman and Company: New York, 1993.
- Freeman, H. C.; Smith, J. E. W. L.; Taylor, J. C. *Acta Crystallogr.* **1961**, *14*, 407.
- Freeman, H. C.; Smith, J. E. W. L.; Taylor, J. C. *Nature* **1959**, *184*, 707.
- Stewart, J. J. P. *J. Mol. Model.* **2007**, *13*, 1173.
- Dreuw, A.; Head-Gordon, M. *Chem. Rev.* **2005**, *105*, 4009.
- Di Marco, V. B.; Bombi, G. G. *Mass Spectrom. Rev.* **2006**, *25*, 347.
- Turecek, F. *Mass Spectrom. Rev.* **2007**, *26*, 563.